Mutual activation of the epithelial-to-mesenchymal transition and metabolic reprogramming stabilizes hybrid phenotypes with high metastatic potential

Madeline Galbraith, Dongya Jia, Herbert Levine, and José Onuchic

Abstract

Abnormal metabolism and metastasis are two hallmarks of cancer. During metastasis, a developmental program, epithelial-to-mesenchymal transition (EMT) has often been used by cancer cells to complete metastasis. Cancer cells undergoing EMT can acquire a hybrid Epithelial/Mesenchymal (E/M) phenotype, which has been shown to be the primary instigator of metastasis. When leaving the primary tumor and entering blood circulation, cancer cells can increase their mitochondrial respiration without compromising their glycolytic activity, thus entering a hybrid metabolic mode using both oxidative phosphorylation (OXPHOS) and glycolysis. Therefore, cancer cells can adjust their metabolic activity for varying metastatic potentials. Understanding the relationship between cancer metabolism and EMT can offer anti-metastasis strategies via targeting metabolism. Here, we analyze the relationship between metabolism and EMT by coupling their corresponding decision-making molecular networks – AMPK/HIF-1/ROS and miR-34/SNAIL/miR-200/ZEB, respectively. We systematically elucidate how different phenotypes during EMT (E, M and hybrid E/M) are associated with different metabolic phenotypes (OXPHOS, glycolysis and hybrid (W/O) glycolysis/OXPHOS). Specifically, we identified the feedback loops that lead to the coupling of the hybrid E/M state with the mixed metabolic state – a potentially highly aggressive phenotype (E/M-W/O). Strikingly, we found that even if the individual molecular network of EMT or metabolism doesn't enable a hybrid phenotype, the crosstalk can promote the existence of a hybrid phenotype. Further, the mutual activation of EMT and metabolic reprogramming occurs

sequentially by first stabilizing the hybrid metabolic phenotype and then the hybrid E/M state, suggesting a potential cause-and-effect relationship between metabolism and EMT; metabolic reprogramming can drive EMT.

Introduction

Metastasis remains the leading cause of cancer-related deaths[1] and thus it is critical to understand the physiological properties of cells that initiate metastatic lesions. Typically, these properties have been studied one at a time. For example, cell motility is assumed to be related to the epithelial-to-mesenchymal transition (EMT). During EMT, the cells progressively lose cell-cell adhesion and apical-basal polarity, and increase their capacity for migration, invasion, and resistance to immune response [2,3]. The EMT has consistently been implicated in cells acquiring metastatic potential [4,5], and also plays a role in therapeutic resistance [6]. Recently, the bimodal picture of EMT has been superseded by a more complex scenario involving the hybrid epithelial/mesenchymal (E/M) phenotype which exhibits combined traits of epithelial (cell-cell adhesion) and mesenchymal (invasion) at the single-cell level. The hybrid E/M cells migrate collectively as a cluster and account for the majority of metastases [7–10]. The existence of a hybrid E/M state has since been experimentally verified both in vitro (many cancer cell lines) and in vivo (using a genetic mouse model of squamous cell carcinoma) and has been shown to be associated with therapy resistance alongside poor survival rates [11–14]. Most importantly, these states appear to the most capable of initiating metastatic growth[15,16]. Fully understanding the behavior of the hybrid E/M phenotype is still an active area of research.

Metabolic reprogramming, another hallmark of cancer, enables cancer cells to adjust their metabolic activity for biomass and energy supply to survive in hostile environments [1,17]. Cells typically utilize oxidative phosphorylation (OXPHOS) under normoxic conditions and glycolysis

when there is a lack of oxygen. However, cancer cells often prefer glycolysis even when oxygen is available, referred to as the Warburg effect or aerobic glycolysis [18,19]. During metastasis, cancer cells must be able to survive in different environments, resulting in these cells switching between different types of metabolism [20–23]. Metabolic reprogramming, specifically in the context of switching between the OXPHOS and Warburg metabolic phenotypes, can lead to mixed metabolic states [24–26] including a metabolic inactive low-low phenotype associated with therapy resistance in melanoma [27] and a hybrid glycolysis/OXPHOS phenotype associated with high metastatic potentials (add refs). The hybrid glycolysis/OXPHOS phenotype has been observed in circulating tumor cells (CTCs) originating from breast tumors formed by 4T-1 cells [28]. The high metastatic potential of cancer cells with a hybrid metabolic phenotype has been confirmed in a number of additional experimental studies (Whether these studies use different cancer cell lines, please elaborate) [29,30].

As already mentioned, most research has focused separately on EMT or metabolic plasticity. However, it has become increasingly clear that there exists extensive crosstalk between EMT and metabolism[30]. The crosstalk between EMT and metabolic reprogramming is important to metastasis and tumor proliferation [30–33]. Recent studies show that metabolic reprogramming can increase metastatic potential and drive EMT, or conversely induction of EMT can drive metabolic reprogramming [34–37]. The underlying mechanisms of interaction between EMT and metabolic reprogramming remain poorly understood, with several competing hypotheses as discussed below. Kang et al have suggested cancer cells typically first undergo metabolic reprogramming then trigger EMT [38]; this coupling, presumably, would account for distinct metabolic needs as cells complete EMT. Another hypothesis is that there is mutual activation of EMT and metabolic reprogramming such that the most flexible (hybrid E/M and

mixed glycolysis/OXPHOS (W/O) phenotype) become coupled, leading to a greatly increased metastatic potential[30]. This connection between EMT and metabolic reprogramming has recently been noticed in CTCs, which were shown to have high levels of both OXPHOS and glycolysis[28] and have also been shown to mainly consist of hybrid E/M cells especially at high levels of NRF2, an antioxidation regulator that upregulates OXPHOS[39]. Consistent coupling of EMT states and metabolic states has been seen in breast cancer stem cells (BCSCs). The hybrid E/M-like BCSCs (E/M-BCSCs) have higher levels of OXPHOS and glycolysis as compared to the mesenchymal-like breast cancer stem cells (M-BCSCs) [40,41]. Thus, while there have been preliminary indications of the coupling of EMT states and metabolic states there is still much to be explored.

To decode the coupled decision-making of EMT and metabolism, we created a computational model which connects the core gene regulatory circuits of EMT – miR34/SNAIL/miR200/ZEB [7] and metabolic reprogramming – AMPK/HIF-1/ROS [25]. We found that ROS is a key promoter of a possible "double-hybrid" state, namely a hybrid E/M state coupled with a mixed metabolic phenotype (hybrid E/M-W/O state). Additionally, HIF-1 may play a more central role in metabolic reprogramming driving EMT than AMPK. Also, when crosstalks between the circuits are active in both directions (EMT regulating metabolism, and vice versa), there are parameter space regions for which the hybrid E/M-W/O state is the only accessible state. Interestingly, if the parameters of the system were modified to exclude the hybrid states when the crosstalks are inactive (i.e., neither the E/M or W/O states are initially accessible), once active, the crosstalks are able to modulate the phase space to generate the hybrid states. In fact, a single crosstalk is sufficient for the metabolic or EMT circuits to gain tristability. We also confirmed the phenotypic stability factors (PSFs) of the hybrid E/M state -

GRHL2 and OVOL2 [14,42] - further stabilized the hybrid E/M-W/O state for all sets of active crosstalks. Our results therefore suggest that a highly aggressive plastic phenotype along both the EMT and metabolic axes is a likely choice for a subset of cancer cells and, speculatively, may be critical for the metastatic process.

Model: Coupling the core EMT and metabolic networks

While the mechanisms of EMT and cancer metabolism have been investigated individually, the crosstalk between the two circuits and how the phenotypes are correlated is still largely unknown. Here we couple our previously studied regulatory networks of EMT [7] and metabolism [25]; see Figure 1A for the coupled network. Generally speaking, our combined model considers the feedback loops that couple the two individual regulatory networks. The crosstalk between the EMT circuit and the metabolism circuit is either direct or indirect, the latter arising because our formulation focuses only on a few core components and effective interactions between them that occur via intermediate reactants. We initially focus on the core networks and investigate the role of crosstalk. One question of interest is whether these crosstalks are sufficient to generate hybrid states. Lastly, we evaluate the role of PSFs OVOL and GRHL2 to investigate their effect on the stability of the E/M-W/O state.

The core EMT network is comprised of the transcription factors (TFs), ZEB and SNAIL, and the microRNA families, μ_{200} and μ_{34}. It is modeled as a translation-transcription chimeric circuit[7]. For a two-component chimeric circuit, the binding/unbinding dynamics are given by

(put the basic equations here)

where the three functions Y_μ, Y_m, and L which represent respectively the active miRNA degradation rate, active mRNA degradation rate, and translation rate (details in SI section 1.2,

Fig. S2-S4). The activation and inhibition of SNAIL and ZEB are mathematically represented as a shifted Hill function,

(shifted hill function)

Once the threshold of the regulator (X_0) is achieved, the fold change (λ) represents the magnitude of the activation ($\lambda > 1$) or inhibition ($\lambda < 1$), and the sensitivity to the changes in X is represented by the Hill coefficient n (details in SI section 1.1, Fig. S1). The previous investigation of the core EMT network by Lu and collaborators examined sub-modules of the network and various parameter ranges. They determined the mir-200/ZEB module was responsible for the tristability of the system whereas the mir-34/SNAIL module acted as a noise buffer[7]. Additionally, the phenotypes of the tristable EMT network were correlated with the expression of mir-200 and ZEB mRNA; epithelial (E) with high mir200/low ZEB, mesenchymal (M) with low mir200/high ZEB, and E/M with intermediate mir-200/ZEB (see Fig. 1A).

The core metabolism network - AMPK/HIF-1/ROS, gave insight into mixed metabolic modes of glucose metabolism. In this circuit, the regulation of the production and degradation terms are mathematically represented as shifted Hill functions. Within the metabolic regulatory network, there is also competitive regulation of ROS by HIF-1 and AMPK which is modeled by a competition function similar to the shifted Hill function (details and functional form in SI section 1.3). Through this reduced circuit, Yu and collaborators were able to recover typical metabolic behavior of cancers and also identify a mixed metabolic (W/O) phenotype[25]. The tristable metabolic network has the metabolic phenotypes; OXPHOS (O) high AMPK/low HIF-1, aerobic glycolysis (W) low AMPK/high HIF-1, and mixed metabolism (W/O) intermediate AMPK/HIF-1 (see Fig. 1B).

To couple the core EMT and metabolic networks we identified crosstalks between our core components (see Fig. 1C). Starting with the miRNA-based crosstalk links, the ability of a cell to eliminate ROS is reduced by μ_{34} via targeting and downregulating the NRF2-dependent antioxidant capability, [43–45]. ROS production may also be upregulated through μ_{34} downregulating SOD2 [46] or via the p53 pathway [47,48]. This increase in ROS levels is potentially more pronounced for mitochondrial ROS (mtROS) versus NADPH oxidase mediated ROS (noxROS) [43] and has recently been indicated as a factor in cancer drug resistance [49]. Next, crosstalk between HIF-1 and μ_{200} family members can either upregulate or downregulate Hif1 expression [50]. While mir-429 upregulates HIF-1, both mir-200b [51] and mir-200c [52] downregulate HIF-1 expression. Furthermore, there is a negative regulatory feedback loop between mir-200b and HIF-1[51]. The inhibition of mir-200b by HIF-1 is indirect, acting through upregulation of the downstream target ASCL2 [51]. Our coupled model includes a mutual inhibitory feedback between μ_{200} and HIF-1. Additionally, HIF-1 can upregulate SNAIL [53]. The production of SNAIL is also a downstream target of AMPK. Once FOXO3 is activated by AMPK, it represses the production of SNAIL[54]. Similarly, Zeb is a downstream target of AMPK, and ZEB production is inhibited by FOXO [55,56]. Additionally, CREB, after being activated by AMPK via phosphorylation, can transcribe μ_{200} resulting in the upregulation of μ_{200}[57–61]. Please refer to supplementary Table S? for a detailed description of all crosstalks.

The new model we propose here is built by including these crosstalk links so as to couple the two core circuits of EMT and metabolic control respectively. The full equations for the dynamics of all components of the circuit are given in SI Section 1.4 and the parameters along with a brief explanation are given in SI Section 1.5.

When the crosstalk links are inactive, there are nine possible couplings of the EMT and metabolic phenotypes: E-W, E-O, E-W/O, M-W, M-O, M-W/O, E/M-W, E/M-O, and E/M-W/O (Fig. 1D, details of simulation in section S2.1). By including active crosstalks, we can identify how the components of the networks interact and which EMT states and metabolic states become coupled.

While the Warburg state is characterized as high HIF-1/low AMPK and the epithelial state is characterized as high μ_{200}/low ZEB mRNA expression, adding the new links will alter the expression profiles for the steady states. This means that the use of fixed thresholds to determine the state of the cell is no longer appropriate. Therefore, we use a distance metric normalized by the expression of the decoupled network to classify the generated expression profiles as one of the nine coupled states (see Section S2.2 for details). With our baseline decoupled network parameters, we show that 1000 initial conditions are large enough to generate consistent percentages of different states (Fig. S6-S8) - with the hybrid state being most populous (W/O and E/M) followed by the W and M phenotypes, followed by the O and E states. This result is just for one set of parameters and others may lead to a different fraction of initial conditions leading to these disparate states.
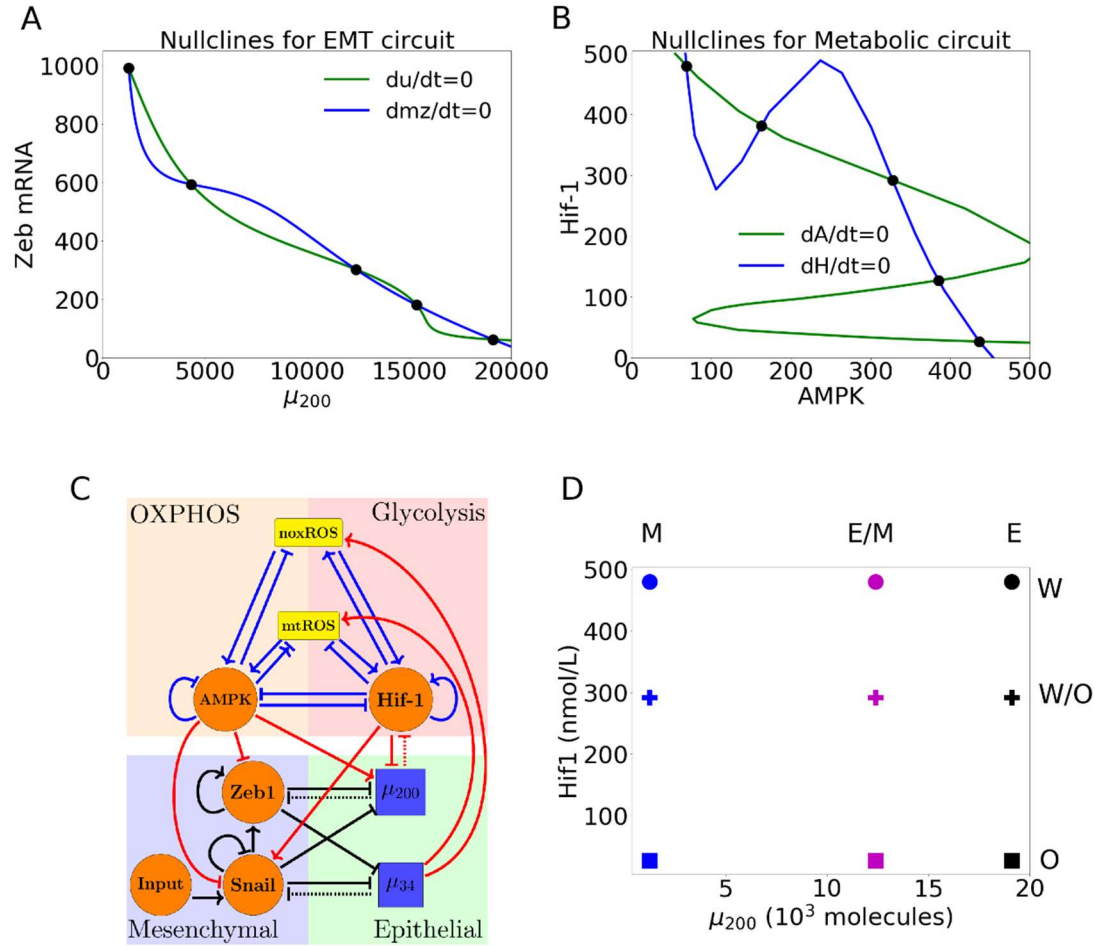
Figure 1. **The coupled EMT/MR circuit results in 9 coupled steady states. (A)** The nullclines of the EMT core network. The system is tristable and the metastable states (high u200/low Zeb mRNA, low u200/high ZEB mrNA, and intermediate u200/ZEB mRNA) correspond to the phenotypes (E, M, E/M). **(B)** The nullclines of the metabolic core network for cancer cells. The system is tristable with metastable states (high AMPK/low HIF-1, low AMPK/high HIF-1, and intermediate AMPK/HIF-1) corresponding to metabolic phenotypes (O, W, W/O). **(C)** The network showing the core EMT module (bottom) with regulatory links designated by black, the core metabolic circuit (top) with regulatory links designated by blue, and the crosstalks noted in red. The dashed lines denote miRNA regulation rather than transcriptional regulation. Regulatory links ending in bars represent inhibition while the arrows represent activation links. **(D)** The 9 possible coupled states when all crosstalks are inactive. The blue, purple, and black markers represent the mesenchymal (M), hybrid epithelial-mesenchymal (E/M), and epithelial (E) steady states, respectively. The circle, cross, and square represent the Warburg (W), hybrid Warburg-OXPHOS (W/O), and OXPHOS (O) metabolic phenotypes, respectively. The coupled E/M-W/O state is therefore represented as a purple cross.

Results

Individual crosstalk can push the downstream circuit towards a single state

Let us start by making just one cross-link active. Now, there is a clearly an unaffected upstream subnetwork (either EMT or metabolism, from where the link originates) and a regulated downstream one.

When noxROS is upregulated by μ_{34} (Fig. 2A), the EMT network remains unaffected while the hybrid W/O state and the coupled E/M-W/O phenotype are upregulated. As the level of noxROS increases (μ_{34} upregulates noxROS by reducing the degredation), the possible coupled states reduce from nine to six, losing first the E-W, then the E/M-W, and finally losing the M-W state (Fig. 2B, section S2.4). Analyzing the percent of initial conditions that lead to the various metabolic phenotypes shows the lost coupled states associated with the Warburg phenotype are pushed towards the W/O phenotype with little change occurring for the OXPHOS associated states (Fig. 2C). As there is no feedback to the EMT network, the percentage of E, E/M, and M states are constant but the E/M state becomes more likely to be associated with the hybrid W/O metabolic phenotype (Fig. 2D). Analyzing the states coupled with the Warburg phenotype, however, shows the mesenchymal phenotype (M-W) persists longer, as expected since it has the lowest μ_{34} level (Fig. 2E). Comparing to the upregulation of mtROS (Fig. S9), the E-W and E/M-W states are also the first suppressed states. Additionally, upregulating mtROS is also correlated with an upregulation of the E/M-W/O phenotype. Further, activation of mtROS results in a downregulation of the OXPHOS metabolic phenotype alongside downregulation of the

Warburg phenotype. Together, these results suggest ROS is critical to tumor progression, and mtROS may play a stronger role than noxROS.
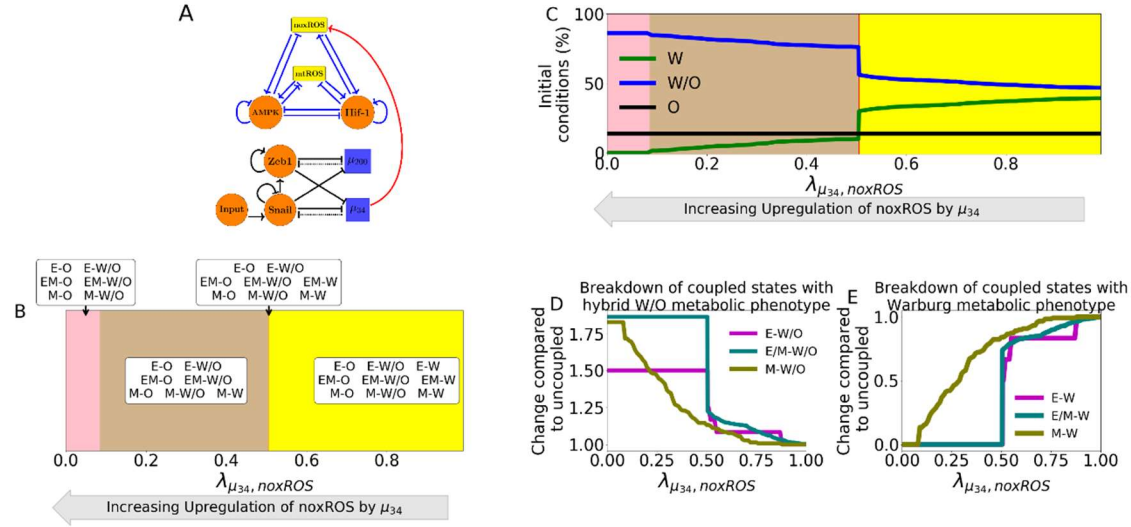

Figure 2. noxROS upregulated by mir34 results in upregulated W/O phenotype and associated with upregulated E/M-W/O phenotype. (A) A diagram of the core EMT circuit (left) and the core metabolic circuit (right) connected by the crosstalk between μ_{34} upregulating noxROS (red link representing transcriptional regulation). **(B)** Of the nine possible coupled states, as noxROS is upregulated by mir34, there are 4 distinct groupings. All possible couplings of the EMT phenotypes (E, M, and E/M) with both the O and W/O metabolic phenotypes persist for all levels of noxROS upregulation. The coupled states associated with the W metabolic phenotypes, (E-W, E/M-W, and M-W), are lost as the level of noxROS regulation increases for the red, tan, and pink regions, respectively. **(C)** The background colors correspond to the colors representing the possible steady states of (B). The lines represent the total number of initial conditions leading to the W, O, or W/O phenotypes as a function of increasing regulation of noxROS by mir34. The W/O phenotype (blue) is upregulated, Warburg (green) phenotype is downregulated, and OXPHOS (black) is unchanged. **(D)** Showing the breakdown of the coupled states associated with the W/O phenotype (i.e., E-W/O, M-W/O, and E/M-W/O) compared to the inactive system ($\lambda_{\mu_{34},noxROS} = 1$). The E/M-W/O coupled state is greatly upregulated once $\lambda_{\mu_{34},noxROS} = 0.5$, the M-W/O coupled state is slowly upregulated, and E-W/O is also upregulated. **(E)** Same as (D) but for the coupled states associated with the Warburg phenotype. Once $\lambda_{\mu_{34},noxROS} = 0.5$, both the E-W and M-W states are fully suppressed. The E/M-W coupled state continues to be downregulated until it is fully suppressed near $\lambda_{\mu_{34},noxROS} = 0.1$.

While u34 crosstalks only affect the downstream network, the miRNA regulation of HIF-1 by u200 can affect both networks. In our model, miRNA regulation is mathematically

represented as three function (Y_m, Y_u, and L) that modify the degradation of HIF-1 mRNA, the

degradation of u200, and the production of HIF-1. Therefore, while the downstream metabolic

network is effected, the upstream EMT network is also affected via degradation of u200

Additionally, these functions have multiple parameters therefore, we use a silencing function

(detail of silencing function $P_H(\mu)$ in section S2.3) that groups subsets of the results based on the

parameters and value of u200. While upregulating ROS pushes the system towards the mixed

W/O metabolic phenotype, when μ_{200} minimally silences HIF-1 mRNA ($P_H(\mu)$ *near* 1) all the

metabolic phenotypes are only coupled to the mesenchymal state. As the silencing increases the

mixed W/O, W, and M states are suppressed, sequentially. When HIF-1 mRNA is fully silenced,

only the E-O and E/M-O coupled states exist (Fig. 3A,). Further, the hybrid E/M-W/O state is

suppressed for all values of μ_{200} silencing Hif-1 mRNA. These results suggest u200

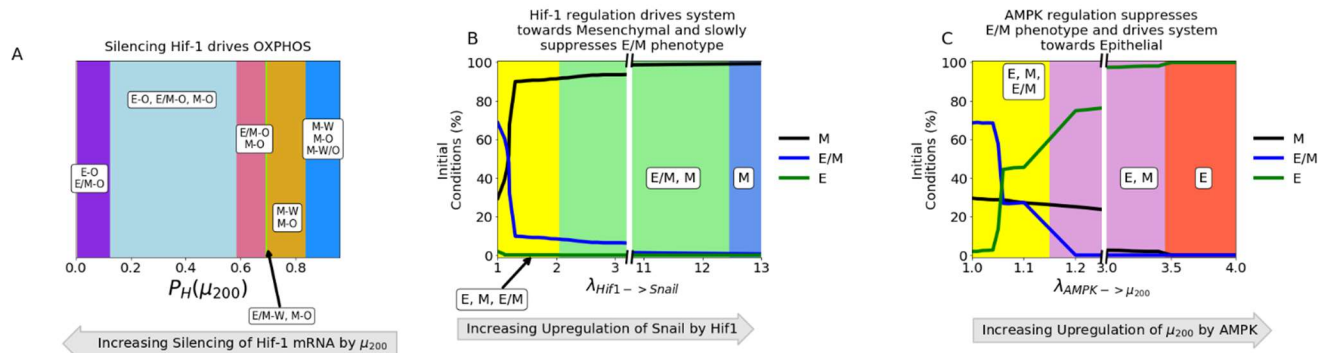overexpression could destabilize the E/M-W/O phenotype.

Figure 3. **(A)** The coupled phenotypes associated with increased silencing of the Hif-1 mRNA by μ_{200}. At minimal silencing ($P_H(\mu_{200})$ near 1) only the coupled states with mesenchymal phenotypes are accessible (M-W, M-O, and M-W/O). Then as silencing increases the mixed metabolic phenotype is lost, then the M-W state becomes E/M-W, and after that only the coupled states with OXPHOS metabolic phenotype are accessible. At complete silencing of the Hif-1 mRNA only the E-O and E/M-O states are accessible. **(B)** The number of initial conditions leading to an E/M, M, or E phenotype as Hif-1 upregulates SNAIL. The hybrid E/M phenotype is suppressed quickly as the system is driven towards mesenchymal. **(C)** Similar to (B) but for AMPK upregulating μ_{200} and driving the system towards epithelial. The E/M state persists longer for Hif-1 regulation than AMPK.

To elucidate the way in which metabolic reprogramming drives EMT, we determine the effect of each metabolism driven crosstalk on the coupled states. First we analyze the crosstalks in which HIF-1 upregulates SNAIL (Fig. 3B and S12) or inhibits μ_{200} (Fig. S13). Both HIF-1 driven crosstalks push the system towards the mesenchymal state. Further, both the epithelial and hybrid E/M states are most associated with the OXPHOS metabolic state while the mesenchymal state is initially associated with the Warburg state. Similarly, modulating the input to SNAIL can alter the presence of the E/M state and increasing the input pushes the system towards mesenchymal (see Fig. S17). Opposite to Hif-1 driven crosstalks, AMPK upregulating u200 pushes the EMT network to adopt an epithelial phenotype and suppresses the E/M state before the mesenchymal state (Fig. 3C and S6). Similarly, AMPK downregulation ZEB or SNAIL has a corresponding effect on the expression of the E/M state and the systems saturate near fully mesenchymal (Fig. S14 and S15). Additionally, if AMPK is regulating the EMT circuit, the epithelial and mesenchymal states are still most associated with the OXPHOS and Warburg metabolic phenotypes, respectively. However, the E/M state for AMPK driven crosstalks is associated with the Warburg state. This is in direct contract to HIF-1 driven crosstalks in which the E/M state is coupled with OXPHOS metabolism. The dependence of the coupled metabolic phenotype on the regulator of the crosstalk link , suggests neither OXPHOS nor Warburg metabolism is strongly associated with the E/M phenotype.

The sets of coupled phenotypes present can be compared between different crosstalks as the regulation is increased. Comparing between noxROS and mtROS upregulation, the E-W and E/M-W coupled states are the first suppressed. Additionally, both crosstalks upregulate the E/M-W/O state, although when mtROS is upregulated only the mesenchymal phenotype is coupled with OXPHOS metabolism. The phases are also very similar whether HIF-1 inhibits u200 or

upregulates Snail. However, the E/M-W/O state does persist longer when HIF-1 inhibits u200 (Fig. S12 and S13). Lastly, the AMPK driven crosstalks are initially very similar. In fact, the phases are nearly identical when AMPK inhibits ZEB or SNAIL (Fig. S14 and S15). However, AMPK upregulating u200 has slightly different phases before saturating at epithelial (Fig. S16). These similarities between crosstalks suggests a preferential pathway exists if EMT drive metabolic reprogramming, or vice versa.

The miRNAs of the EMT network can stabilize the W/O metabolic phenotype

We next wish to determine how including links emanating from both miRNAs of the EMT network can drive metabolic reprogramming, and specifically enhance the chances of being in the E/M-W/O state. As mentioned previously, upregulated ROS leads to an increased W/O phenotype (Fig. S9). If both noxROS and mtROS are upregulated by μ_{34} the E/M-W/O state is further upregulated (Fig. S11). While upregulation of ROS causes an increase in the hybrid E/M-W/O, μ_{200} silencing HIF-1 mRNA suppresses the hybrid E/M-W/O state; therefore, some suppression of the hybrid E/M-W/O state is expected when u200 and u34 regulate HIF-1 and ROS, respectively. Interestingly, the hybrid E/M-W/O state is fully suppressed when μ_{200} downregulates HIF-1 and μ_{34} upregulates noxROS, but only partially suppressed when μ_{200} downregulates HIF-1 and μ_{34} upregulates mtROS (Fig. S10). These results suggest the type of ROS present can affect expression of the E/M-W/O state.

The hybrid E/M-W/O state is stabilized if mtROS is upregulated, but noxROS upregulation has minimal affect on the hybrid E/M-W/O state. Strikingly, if all three miRNA crosstalks are active (μ_{200} silencing HIF-1 mRNA and μ_{34} upregulating noxROS and mtROS, Fig. 4A) the E/M-W/O coupled state may be suppressed even if the W/O state is present (Fig.

4B). Further, the E/M-W/O phenotype is present for all values of noxROS upregulation but is only present at high values of mtROS upregulation (Fig. 4B). Analyzing the coupled state phases) shows the E/M-W/O state is suppressed when mtROS is only slightly upregulated (Fig. 4C. For the entire phase space see Fig. S19A). Further, the epithelial and E/M states are associated with the OXPHOS phenotype when mtROS levels are slightly upregulated. Interestingly, the mesenchymal state is coupled with O and W/O metabolic phenotypes while the E and E/M states are only coupled to the W/O phenotype when mtROS is fully upregulated. Additionally, depending on the initial conditions, if noxROS is maximally upregulated, mtROS is upregulated, and HIF-1 is partially silenced by u200 the system can access the hybrid E/M-W/O state (Fig 4D). Also, while mtROS must be upregulated for the system to access the E/M-W/O state, the hybrid state is accessible for all levels of noxROS upregulation (SI Fig S?). The difference in the effect of noxROS and mtROS seems to result from the frustrated regulation on mtROS by HIF-1 and u34. Therefore, a feedback look between mtROS, HIF-1, u34, and u200 may control the expression of the E/M-W/O state.
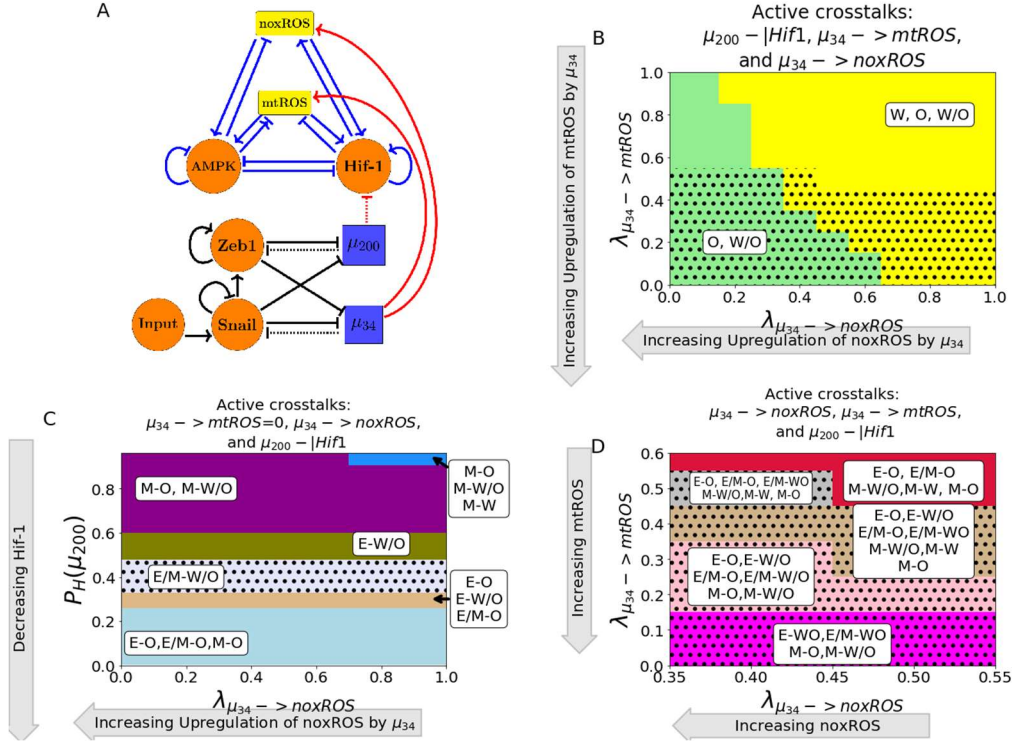
Figure 4. miRNA of the EMT regulatory network can upregulate the W/O phenotype. (A)
The coupled metabolic (top) and EMT (bottom) regulatory network with all EMT driven
regulatory links active (μ_{34} upregulating mtROS, μ_{34} upregulating noxROS, and μ_{200} silencing
Hif-1). **(B)** The phase plane corresponding to all EMT driven regulatory links (network pictured
in A). The regulation of Hif-1 by μ_{200} in this phase plane corresponds to the blue region of Fig. 3
where all metabolic phenotypes are possible. As noxROS is upregulated (right to left), the
Warburg metabolic phenotype is suppressed. However, as the level of mtROS increases (top to
bottom), the black dotted region appears showing the existence of the E/M-W/O coupled state,
suggesting mtROS may have a stronger affect on the E/M-W/O phenotype than noxROS. **(C)**
The coupled states when only EMT driven crosstalks are active (μ_{200} downregulating HIF-1 and
μ_{34} upregulating mtROS and noxROS). The E/M-W/O state exists when mtROS is upregulated.
(D) At maximum upregulation of noxROS ($\lambda_{\mu_{34}->noxROS}=0$), as mtROS increases (x-axis) and
Hif-1 is silenced (y-axis) there are regions where the E/M-W/O state is possible (black dotted
regions).

TFs of the metabolic network can stabilize the E/M metabolic phenotype

There are two distinct events at play when the metabolic network regulates the EMT

circuit. AMPK regulation quickly suppresses the E/M phenotype and pushes the system towards

the Epithelial state whereas HIF-1 regulation can allow the system to maintain the E/M

phenotype while ultimately pushing the system towards mesenchymal (Fig. 3B and 3C). As AMPK and HIF-1 push the system towards opposite states, having one active link drive by each would suggest the circuit could be pushed towards a hybrid state. That is exactly what happens for any combination of the three AMPK crosstalks and two HIF-1 crosstalks, although the exact values of where the E/M-W/O state exists depends on the type of regulation (Fig. S18). Additionally, if AMPK and Hif-1 target different EMT TFs, the E/M-W/O state may exist in more regions than if they target the same TF (Fig. S18), suggesting multiple crosstalks must be active and multiple gene regulators must be targeted to stabilize the E/M-W/O state. If all crosstalks involving AMPK and HIF-1 regulating the EMT circuit are active (Fig. 5A) then there are regions in which the E/M state exists (Fig. 5B). However, when analyzing the system for the existence of the E/M-W/O phenotype, it only exists in a small region when u200 is minimally upregulated. Moreover, HIF-1 driven crosstalks are able to maintain the E/M phenotype longer than AMPK driven crosstalks suggesting, the reduced regions of E/M-W/O existence is likely due to the suppression of the E/M state by AMPK regulated crosstalks, as mentioned above (see Fig. S14-S16). This suggests HIF-1 driven crosstalks may be more tumorigenic than AMPK driven crosstalks.

To stabilize the E/M state an AMPK and HIF-1 crosstalk are necessary, and if all EMT regulating crosstalks are active then there are regions where the E/M-W/O state exists. Additionally, the epithelial state is typically coupled to OXPHOS metabolism (E-O), the mesenchymal state is associated with the Warburg metabolic phenotype (M-W), and when the E/M state is present it is typically associated with the hybrid W/O metabolic phenotype (Fig. 5C and S19B). In fact, for any system, if there are only three coupled states available and each has a distinct phenotype of the EMT and metabolic networks then the only possible set of states is E-

O, M-W, and E/M-W/O. This suggests, cells in the primary tumor utilize OXPHOS while

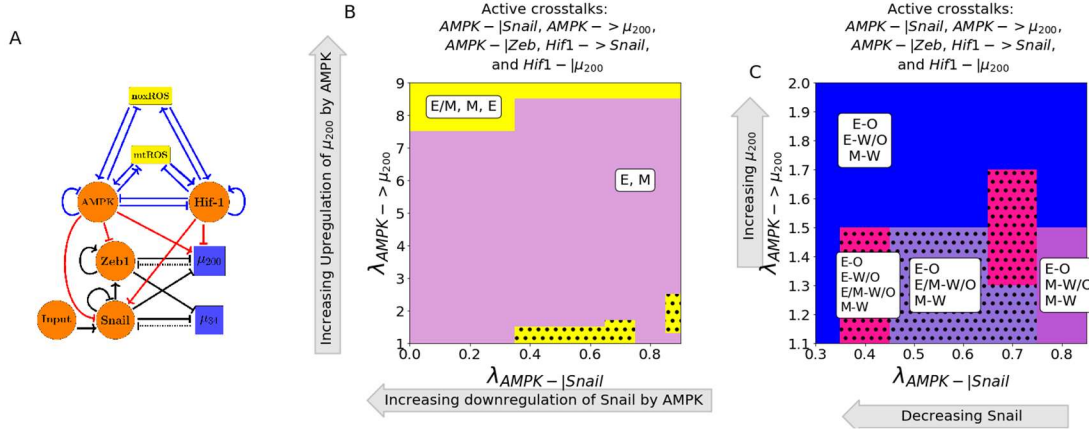clusters of migrating cells utilize a combination of aerobic glycolysis and OXPHOS.

Figure 5. AMPK and Hif-1 cooperate to upregulate the hybrid E/M state. (A) The network showing metabolism driven crosstalks. ZEB is inhibited by AMPK, SNAIL is upregulated by Hif-1 while being downregulated by AMPK, and μ_{200} is upregulated by AMPK while being inhibited by Hif-1. **(B)** The phases plane of potential EMT phenotypes when all metabolic driven crosstalks are active. The E/M phenotype is only accessible when $\lambda_{AMPK-|\mu200}$ is near 1 or very high (i.e., at the extremes of regulation). **(C)** The coupled states when only TFs and miRNAs of the EMT circuit are regulated by TFs of the metabolic circuit (AMPK-|SNAIL, AMPK-|ZEB, AMPK->u200, HIF-1 -|u200, HIF-1 -> SNAIL). The results suggest a correlation between the E, E/M, and M phenotypes to the O, W/O, and W metabolic phenotypes.

The Hybrid E/M-W/O phenotype

    As the most aggressive cancers phenotypes are characterized by the hybrid E/M state and

mixed metabolism, we narrow our search onto how the crosstalks in both directions affect the

presence of the E/M-W/O state and the behavior of the coupled states as the regulatory crosstalks

change. Further, the E/M-W/O state is present for some regions of the phase plane when all EMT

driven crosstalks are active or all metabolic driven crosstalks are active, the hybrid E/M-W/O

state can also be suppressed. Therefore, a metabolic driven crosstalk and two competing EMT

driven crosstalks would be minimally necessary to fully stabilize the E/M-W/O state and suppress all other coupled states.

The hybrid E/M-W/O state can be upregulated when AMPK downregulates SNAIL, HIF-1 downregulates u200, and u34 upregulates mtROS. The E/M-W/O phenotype exists in much of the space and is upregulated when the downregulation of SNAIL by AMPK has pushed the system to be in the nearly mesenchymal regime ($\lambda_{AMPK-|SNAIL}=0.2$), mtROS is increased, and u200 levels have decreased (Fig 6A). Further, instead of HIF-1 downregulating u200, the Input to SNAIL can be increased, causing the E/M-W/O state to be upregulated again (Fig. 6B). While, the E/M-W/O state was upregulated in both cases, neither was able to fully stabilize the E/M-W/O state and suppress all other states.

It is possible to suppress all states except the hybrid E/M-W/O state with just three regulations; HIF-1 inhibiting μ_{200}, μ_{34} upregulating mtROS, and modulating the input to SNAIL (Fig. 6C and S19C). Further, no other combination consisting of only three regulatory links seems to suppress all states except the E/M-W/O state, even if a crosstalk is replaced by modulating the input to SNAIL. Additionally, this region which only includes the E/M-W/O state persists even if all crosstalks are active (Fig. 6D and S19D).

The proximal phases suggest stabilization of the E/M-W/O state is driven by mutual activation of metabolic reprogramming and EMT. When the E/M-W/O state is the only one available (Fig. 6C and 6D), the nearby phases are the same whether three crosstalks or all crosstalks are active (E-O and E-W/O), suggesting there is a progression that must be followed to generate the E/M-W/O state. Further, if the E/M-W/O state is only upregulated (Fig. 6A and 6B), the surround phases include mesenchymal coupled states (M-O, M-W/O, and M-W) as well as

(E-O and E-W/O). This suggests first metabolic reprogramming occurs (E-W/O) followed by a partial EMT (E/M-W/O). Consequently, this suggests the system can only fully transition to E/M-W/O if the cells are initially in the E-O state. Additionally, the persistence of the E/M-W/O state suggests there are other combinations of crosstalks that generate phases where only the E/M-W/O state is possible, although it is outside the scope of this manuscript to find all possible combinations of crosstalks that can suppress all states except the hybrid E/M-W/O coupled state. However, based on these results, we would expect HIF-1 suppressing u200 and u34 upregulating mtROS to be prominent among all such combinations.
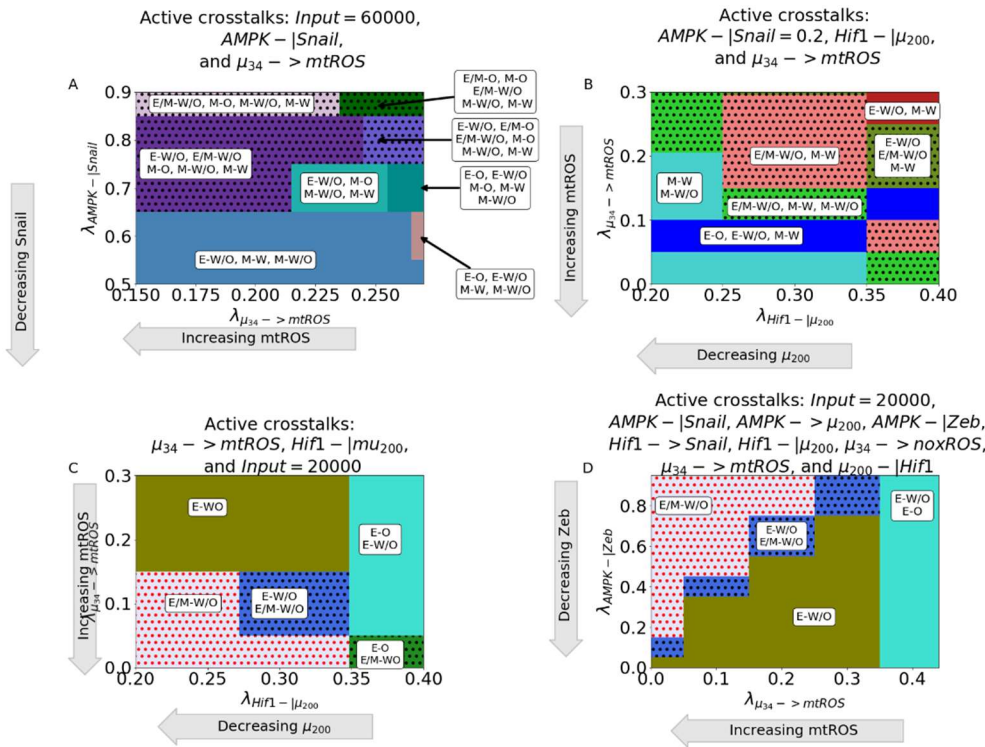

Figure 6. The EMT and metabolic regulatory networks crosstalks can drive the system to the hybrid E/M-W/O coupled state. (A) The coupled states when the Input=60000, AMPK downregulates Snail, and u34 upregulates mtROS. The E/M-W/O state is upregulated when mtROS levels are increased. **(B)** The phase plane when $\lambda_{AMPK-|SNAIL}$=0.2, HIF-1 inhibits μ_{200} production, and u34 upregulates mtROS. The E/M-W/O state is upregulated for some regions. **(C)** When crosstalks mutually drive EMT and metabolic reprogramming, there are parameter spaces in which the only possible coupled state is the E/M-W/O state. **(D)** When all crosstalks are active there are regions where only the E/M-W/O state exists. Similar sets of coupled states

in (C) and (D) suggest a preferential pathway to drive the system towards the hybrid E/M-W/O coupled state.

Normal cells can become cancerous when crosstalks introduced

We have confirmed the E/M and W/O states are coupled, the E/M-W/O state can be upregulated, and there are parameter sets with only the hybrid E/M-W/O state available and all other coupled states suppressed. However, these results are for a network model in the parameter regime of cancer cells (i.e., tristable circuits with a hybrid intermediate state). To determine whether EMT can drive metabolic reprogramming, and vice versa, we modify the network to be in the parameter regime of normal cells (i.e., bistable systems with no hybrid state). A few key parameters were modified to affect SNAIL regulating u200, SNAIL regulating ZEB, HIF-1 degradation, HIF-1 mRNA degradation, and the competitive regulation of mtROS by AMPK and HIF-1 (see Section S1.6 for parameters). We confirmed both the EMT and metabolic networks are independently bistable when the crossstalks are inactive by calculating the nullclines for the system (Fig. S20) and ensured the solutions from the initial conditions were evenly divided between the steady states (Fig. S21-S22). Now we determine if EMT can drive metabolic reprogramming, metabolic reprogramming can drive EMT, and whether there is a preference when the crosstalks are active but both networks are bistable.

The EMT network can drive metabolic reprogramming if u34 upregulates mtROS. We keep the EMT circuit as the tristable network but change the parameters of the metabolic circuit to reflect normal cells (i.e., no hybrid W/O state in the inactive network). Then we analyze the coupled phenotypes when either u34 upregulates mtROS, u200 downregulates HIF-1, or u34 upregulates noxROS. The metabolic circuit only becomes tristable (generates the mixed W/O

phenotype) at high levels of mtROS upregulation (Fig. 7A). Additionally, when μ_{34} activates mtROS it can even upregulate the E/M-W/O stateso that all E/M phenotypes are coupled with the hybrid metabolic W/O phenotype. However, the system remains bistable and the hybrid metabolic phenotype is not generated if only noxROS is upregulated or μ200 is downregulated (Fig. S23). Interestingly, minimal change occurs for the coupled phenotypes when u200 silences HIF-1 mRNA, suggesting this crosstalk may be anti-tumorigenic. Furthermore, the upregulation of noxROS in the bistable circuit causes an increase in OXPHOS metabolism, in contrast to an increase of the hybrid W/O state in the tristable circuit. This suggests, noxROS may play a pro- or anti-tumorigenic role depending on the system, unlike mtROS which can stabilize the E/M-W/O phenotype.

Metabolic reprogramming can drive EMT if HIF-1 controlled crosstalks are active. Opposite to the above, we keep the metabolic circuit as a tristable circuit and modify the EMT network to be bistable (i.e., no hybrid E/M state in the inactive network). Then we investigate the effects as a single crosstalk is turned on. When HIF-1 inhibits u200, the system is able to quickly generate the E/M-W/O state before it is once again suppressed (Fig. 7B). However, the E/M phenotype persists but is coupled to the OXPHOS metabolic phenotype (E/M-O). Additionally, when HIF-1 upregulates SNAIL the E/M-W/O state is only generated at low levels of SNAIL upregulation (Fig. S24). Furthermore, both systems saturate near mesenchymal while maintain the hybrid E/M phenotype (E/M-O, M-W, M-O, M-W/O). This suggests the master regulator of metabolic reprogramming, HIF-1, can drive normal cells towards the E/M phenotype. Conversely, an individual AMPK driven crosstalk is unable to generate the hybrid E/M state and saturates near the fully epithelial phase (Fig. S24), as seen in the tristable circuit. Additionally, as with the tristable networks, the hybrid E/M-W/O state can be stabilized if two competing

crosstalks, such as AMPK upregulating SNAIL and Hif-1 downregulating μ_{200} (Fig. S25), and the E/M-W/O state is stabilized for larger parameter regions that either crosstalk generates individually. These results suggest HIF-1 can strongly affect and drive EMT while AMPK can only help stabilize the E/M-W/O state if it is already present.

When both networks are in the parameter regime of normal cells (i.e., no E/M or W/O states are present for the inactive crosstalks), metabolic reprogramming drives EMT. For the tristable circuit, the simplest set of crosstalks with a parameter region that suppressed all coupled states except the E/M-W/O state included the three regulations;Hif-1 inhibiting μ_{200}, μ_{34} upregulating mtROS, and modulating the input to SNAIL. When these same links are active for the bistable circuit the results are qualitatively very similar to the tristable circuit results (Fig. 7C and S26 compared to Fig. 6C). The E/M state is only possible near full inhibition of μ_{200} and the W/O state is possible when mtROS greatly upregulated. Further, the system must be near maximum regulation (i.e. both foldchanges must be close to zero) to generate the region where only the hybrid E/M-W/O coupled state is possible. Additionally, the nearby phases correspond to the phases of the tristable circuit (E-O and E-W/O), further supporting the existence of a preferential pathway that stabilizes the E/M-W/O state and follows intuition. As EMT starts with an epithelial state, and knowing the epithelial state typically uses OXPHOS, the transition from E-O to E-W/O to E/M-W/O suggests metabolism may help drive EMT given the metabolism must first be reprogrammed to hybrid W/O which then drives the beginning of EMT and stabilizes the hybrid E/M state. These results also confirm a mutual activation between EMT and metabolic reprogramming.
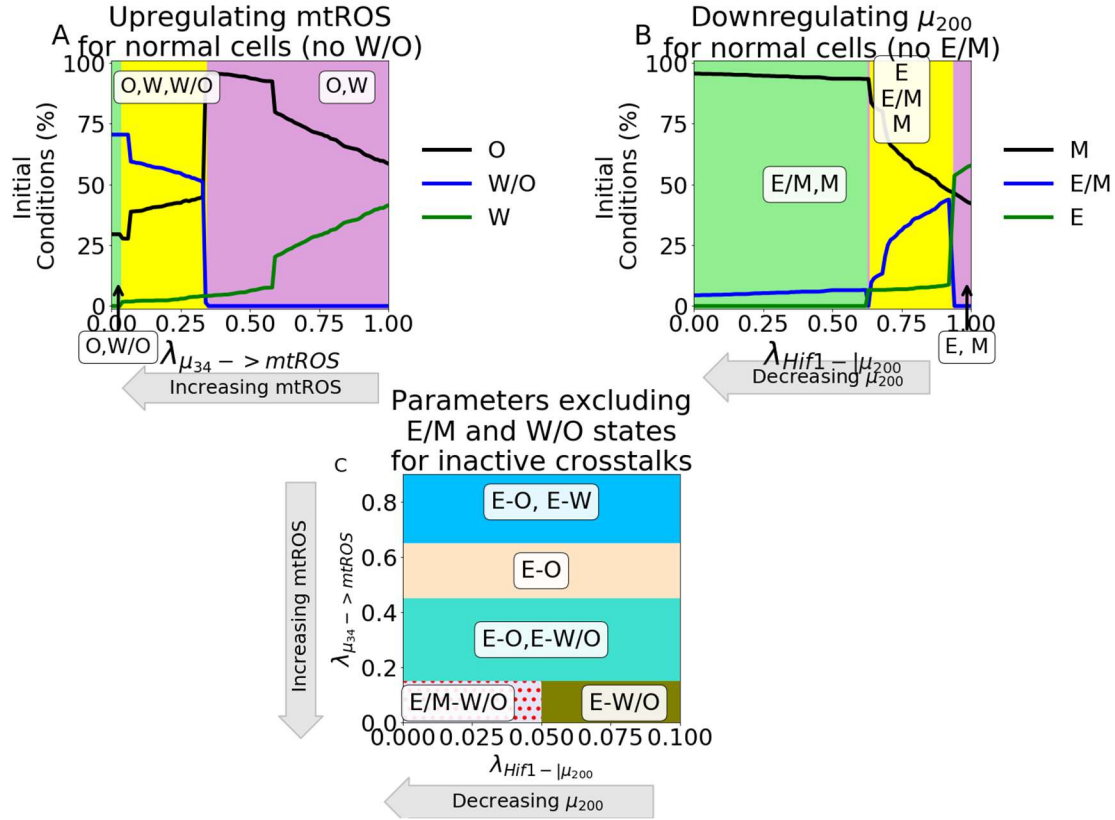
Figure 7. Parameter ranges which exclude the possibility of the hybrid state can be modulated by crosstalk to generate the hybrid state. (A) Our model using parameters that remove the hybrid W/O metabolic state from the steady state possibilities when the crosstalk is inactive ($\lambda_{\mu_{34}->mtR}$ $= 1.$). Initially, only the OXPHOS and Warburg metabolic states can be accessed with an increase in the percent of OXPHOS steady states and decrease in Warburg phenotypes. Once $\lambda_{\mu_{34}} = 0.35$, there is a sharp change with the hybrid W/O phenotype becoming the most often occupied phenotype. **(B)** Our model using parameters that remove the hybrid E/M phenotype from the accessible states when the crosstalks are inactive. As the inhibition increases ($\lambda_{Hif1-|\mu_{200}}$ goes towards zero), the system goes from only the E and M states available to regions in which the E/M phenotype is accessible. **(C)** Combining the models from (A) and (B), we generate a model which only has 4 possible coupled states if the crosstalks are inactive (E-O, E-W, M-O, and M-W). At maximum upregulation of mtROS and downregulation of μ_{200}, the E/M-W/O state is the only one accessible, similar to the model with parameters always allowing access to the E/M-W/O state (Fig. 6C).

PSFs can stabilize the hybrid E/M-W/O state

Lastly, we investigate the effects of the crosstalks when the system is already stabilized in the E/M-W/O hybrid state. The PSFs GRHL2 and OVOL are known to stabilize the hybrid E/M state[14,42]. Also, GRHL2 upregulates ROS in a manner similar to u34[62], GRHL2

should stabilize the W/O phenotype. Therefore, we modify the original tristable network to include the PSFs (parameters and modified equations of the PSF stabilized network are in Section S1.7). When the crosstalks are inactive, we find the PSF stabilized network can either be in the E/M-W/O or E/M-O state, and more than 90% of initial conditions lead to the hybrid E/M-W/O state (Fig. S27).

When a single crosstalk is active in the PSF coupled network, the behavior is as expected with the E/M-W/O state persisting for more values than the tristable coupled network. For instance, the hybrid E/M-W/O state is stabilized at all values of the foldchange for AMPK downregulating SNAIL, AMPK upregulation u200, and u34 upregulating noxROS (see Fig. S28). However, when HIF-1 downregulates u200 or HIF-1 upregulates SNAIL, the E/M-W/O state is only stabilized for some values of the foldchange, but the E/M-W/O is present for more values when PSFs stabilize the circuit compared to the original tristable network (Fig. S28). These results confirm the PSFs increase the stability of the E/M-W/O state, even in when crosstalks are active.

When multiple crosstalks are active the stability of the E/M-W/O state persists. If two competing crosstalks on the EMT circuit are active (i.e., one Hif-1 and one AMPK driven regulation active), then the E/M-W/O state is possible for most of the parameter space (Fig. 8B). The regulatory crosstalks controlled by HIF-1 seem to have a stronger affect than the AMPK crosstalks and can push the system towards mesenchymal, as shown by the presence of the M-W/O state as u200 is inhibited by HIF-1. This corresponds with results from the tristable and bistable coupled networks where AMPK upregulating μ_{200} seems to have a weaker effect, specifically on the stability of the E/M-W/O state, than HIF-1 downregulating μ_{200}. Lastly, we activate the three crosstalks that were shown in the tristable and bistable networks to suppress all

states except the E/M-W/O state; μ_{34} upregulates mtROS, HIF-1 downregulates μ_{200}, and the input to SNAIL is modulated. Once again, there is a phase where only the E/M-W/O state exists. Furthermore, the phase exists in a far larger region when stabilized by the PSFs than for the corresponding tristable or bistable coupled network (Fig. 8C and S29). Specifically, the light red region at the bottom left corner of Fig. 8D, shows the parameter space where the E/M-W/O state is the only one available for the tristable network at this level of input to Snail. The large red region surrounding it is the additional parameter space the E/M-W/O state is stabilized in when the PSFs are coupled with the network. Further, the states in the phases surrounding the region of E/M-W/O stability are the same as the bistable networks (E-W/O and E-O), and also correspond to those of the tristable network. Thus, incorporating the PSFs – GRHL2 and OVOL – can increase the stability of the E/M-W/O state and agree with our previous finding of mutual activation between the EMT and metabolic networks.
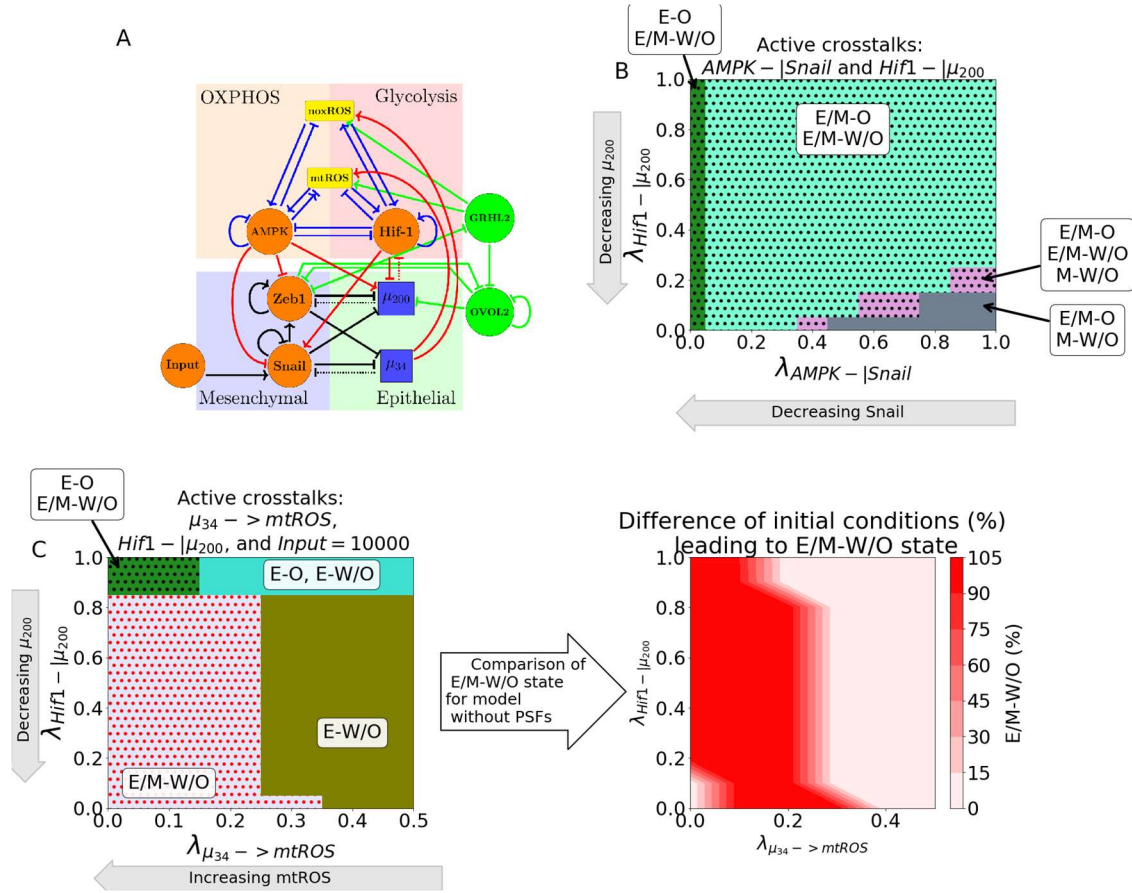
Figure 8. PSFs stabilizing E/M state can increase parameters spaces of E/M-W/O states. **(A)** The modified network to include GRHL2 and OVOL2. **(B)** The coupled E/M-W/O state is present in more of the space due to the PSFs stabilizing the E/M state even when AMPK downregulates SNAIL and HIF-1downregulates μ_{200}. **(C)** The phase space when the Input to SNAIL is set to 10K, μ_{34} is upregulating mtROS, and HIF-1 is downregulating μ_{200}. There is a larger regions where the E/M-W/O state is the only possible coupled state compared to the original model. **(D)** The difference in the percent of initial conditions between (C) and the original model when the input to SNAIL is 10K, μ_{34}upregulates mtROS, and HIF-1 inhibits μ_{200}. The dark red region shows the area in which the PSF stabilized model only has the E/M-W/O state. The light red in the bottom left corner near (0,0.1) is the only region in which both models are fully in the E/M-W/O state. The light red on the right is where neither model is in the E/M-W/O state.

Discussion

Based on this work we have seen that there does seem to be a link between the hybrid

E/M and W/O states suggesting that metastasizing cells require a hybrid metabolic approach to

increase their rate of energy production. We have identified some crosstalks that could be expanded upon to increase our understanding of metastasis.

mtROS nearly suppressing the OXPHOS and Warburg phenotypes combined with the results that the upregulation of the EM/WO state is more pronounced for mtROS than noxROS[43] suggests mtROS specifically is critical to tumor progression. This finding is supported by recent experimental work by Radisky and collaborators that identifies ROS as a potential driver of the epithelial to mesenchymal transition [63]. The role of μ_{34} upregulating ROS to trigger the hybrid metabolic W/O phenotype and the role of μ_{200} downregulation in stabilizing the E/M-WO state corresponds with the importance of miRNAs in cancer metastasis [64]. Additionally, the metabolic transcription factor HIF-1 is important in metabolic reprogramming [22], and our results show, in combination with other crosstalks, HIF-1 can stabilize the E/M-W/O. Our results showing the importance of the HIF-1/mtROS axis agree with previous experimental results[65]. The role of HIF-1 stabilizing the E/M-W/O state, combined with HIF-1 crosstalks having a stronger affect than AMPK on EMT, corresponds to the well-known role of hypoxia, and metabolic reprogramming, triggering EMT [9]. Consequently, our results suggest the existence of a feedback loop between μ_{34}, μ_{200}, HIF-1 and ROS that may be critical to stabilizing the E/M-W/O state associated with tumorigenesis.

The feedback loop, especially μ_{34} upregulating ROS, may be of critical importance given the p53 and KEAP1-NRF2 pathways may have competing effects on EMT and metabolism. For instance, there is a connection between NRF2 upregulation and the E/M phenotype [39] but NRF2 is also an antioxidant that must be downregulated to upregulate ROS production [43–45]. However, the metabolic phenotype of NRF2 stabilized E/M cells may correspond to a hybrid W/O phenotype [28]. Additionally, the p53 pathway seems to upregulate noxROS, and therefore

the W/O phenotype, even though the upregulation of p53 is known to be anti-tumorigenic [47,48]. Here we establish a connection between ROS upregulation and the E/M-W/O phenotype, and to further elucidate the mechanism by which ROS promotes tumorigenesis, additional pathways such as the KEAP1-NRF2 and p53 pathways should also be explored in conjunction with crosstalks between the EMT and metabolic circuits. Additionally, the E/M-W/O state was stabilized when the input to SNAIL was modulated confirming the tumor microenvironment and other signals, such as TGF-β and NF-$\kappa\beta$, may be important to generating the E/M-W/O state [66,67].

Understanding how the E/M-W/O phenotype is stabilized by the crosstalks of EMT and metabolic reprogramming is of vital importance to disrupt metastatic processes. While EMT seems to be able to stabilize metabolically advantageous phenotypes, like the hybrid W/O state, more evidence seems to support metabolic reprogramming drives EMT, especially regarding OXPHOS and glycolysis[32,38,68]. Our results suggest not only does metabolic reprogramming drive EMT, but metabolic reprogramming is not completed before EMT begins which allows the most aggressive E/M-W/O phenotype to stabilize. Further, to ensure only the E/M-W/O state is accessible, the system seems to first require the E-O state, seen in most cells of the primary tumor[69]. Then the cells undergo metabolic reprogramming while maintaining the epithelial characteristics (E-W/O coupled state). Lastly, cells begin EMT and stabilize in the E/M-W/O state, suggesting EMT and metabolic reprogramming are strongly correlated. Strikingly, the E/M-W/O state is upregulated by these crosstalks regardless of phenotypic availability (i.e., whether the initial system is fully E/M-W/O or only E-O, E-W, M-O, and M-W) , suggesting the crosstalks involved in tumorigenesis have evolved to ensure survival and proliferation. The

importance of this feedback loop could be experimentally tested by reducing the antioxidant factor SOD2, inducing hypoxia, and treating the cells with NF-κβ.

Given the interplay between metabolic reprogramming and EMT, some therapeutic approaches target metabolic processes to inhibit growth while also targeting metabolic pathways known to drive EMT[31,32,70]. Further, many drugs that inhibit metabolic pathways of cancers have been shown to inhibit EMT [70]. Although these therapeutics are promising, we have shown that the EMT and metabolic network mutually drive the E/M-W/O phenotype; therefore, therapeutic approaches should be developed to ensure EMT and metabolism are directly targeted, either through a combination therapy or a drug that has targets in both networks. Additionally, current works suggest targeting multiple metabolic pathways is advantageous[71]. Therefore, identifying targets of other metabolic pathways that drive EMT may be important to future therapies. This would also confirm whether the type of metabolism can alter the preference of metabolic reprogramming to drive EMT. Further, potential therapeutics should be tested to ensure they do not upregulate EMT or other metabolic pathways.

1. Hanahan D. Hallmarks of Cancer: New Dimensions. Cancer Discov. 2022;12(1):31–46.

2. Kalluri R. EMT: When epithelial cells decide to become mesenchymal-like cells. J Clin Invest. 2009;119(6):1417–9.

3. Hay ED. The mesenchymal cell, its role in the embryo, and the remarkable signaling mechanisms that create it. Dev Dynam. 2005;233(3):706–20.

4. Pietilä M, Ivaska J, Mani SA. Whom to blame for metastasis, the epithelial–mesenchymal transition or the tumor microenvironment? Cancer Lett. 2016;380(1):359–68.

5. Talbot LJ, Bhattacharya SD, Kuo PC. Epithelial-mesenchymal transition, the tumor microenvironment, and metastatic behavior of epithelial malignancies. Int J Biochem Mol Biol. 2012 May 18;3(2):117–36.

6. Cho ES, Kang HE, Kim NH, Yook JI. Therapeutic implications of cancer epithelial-mesenchymal transition (EMT). Arch Pharm Res. 2019;42(1):14–24.

7. Lu M, Jolly MK, Levine H, Onuchic JN, Ben-Jacob E. MicroRNA-based regulation of epithelial–hybrid–mesenchymal fate determination. Proc National Acad Sci. 2013;110(45):18144–9.

8. Saitoh M. Involvement of partial EMT in cancer progression. J Biochem. 2018;164(4):257–64.

9. Saxena K, Jolly MK, Balamurugan K. Hypoxia, partial EMT and collective migration: Emerging culprits in metastasis. Transl Oncol. 2020;13(11):100845.

10. Bakir B, Chiarella AM, Pitarresi JR, Rustgi AK. EMT, MET, Plasticity, and Tumor Metastasis. Trends Cell Biol. 2020;30(10):764–76.

11. Pastushenko I, Blanpain C. EMT Transition States during Tumor Progression and Metastasis. Trends Cell Biol. 2018;29(3):212–26.

12. Fustaino V, Presutti D, Colombo T, Cardinali B, Papoff G, Brandi R, et al. Characterization of epithelial-mesenchymal transition intermediate/hybrid phenotypes associated to resistance to EGFR inhibitors in non-small cell lung cancer cell lines. Oncotarget. 2017;8(61):103340–63.

13. George JT, Jolly MK, Xu J, Somarelli J, Levine H. Survival outcomes in cancer patients predicted by a partial EMT gene expression scoring metric. Cancer Res. 2017;77(22):canres.3521.2016.

14. Jolly MK, Tripathi SC, Jia D, Mooney SM, Celiktas M, Hanash SM, et al. Stability of the hybrid epithelial/mesenchymal phenotype. Oncotarget. 2016;7(19):27067–84.

15. Pastushenko I, Brisebarre A, Sifrim A, Fioramonti M, Revenco T, Boumahdi S, et al. Identification of the tumour transition states occurring during EMT. Nature. 2018;556(7702):463–8.

16. Simeonov KP, Byrns CN, Clark ML, Norgard RJ, Martin B, Stanger BZ, et al. Single-cell lineage tracing of metastatic cancer reveals selection of hybrid EMT states. Cancer Cell. 2021;39(8):1150-1162.e9.

17. Dey P, Kimmelman AC, DePinho RA. Metabolic Codependencies in the Tumor Microenvironment. Cancer Discov. 2021;candisc.1211.2020.

18. Warburg O, Wind F, Negelein E. THE METABOLISM OF TUMORS IN THE BODY. J Gen Physiol. 1927;8(6):519–30.

19. Liberti MV, Locasale JW. The Warburg Effect: How Does it Benefit Cancer Cells? Trends Biochem Sci. 2016;41(3):211–8.

20. Ohshima K, Morii E. Metabolic Reprogramming of Cancer Cells during Tumor Progression and Metastasis. Metabolites. 2021;11(1):28.

21. Carvalho TMA, Cardoso HJ, Figueira MI, Vaz CV, Socorro S. The peculiarities of cancer cell metabolism: A route to metastasization and a target for therapy. Eur J Med Chem. 2019;171:343–63.

22. Nagao A, Kobayashi M, Koyasu S, Chow CCT, Harada H. HIF-1-Dependent Reprogramming of Glucose Metabolic Pathway of Cancer Cells and Its Therapeutic Significance. Int J Mol Sci. 2019;20(2):238.

23. Cheng Y, Lu Y, Zhang D, Lian S, Liang H, Ye Y, et al. Metastatic cancer cells compensate for low energy supplies in hostile microenvironments with bioenergetic adaptation and metabolic reprogramming. Int J Oncol. 2018;53(6):2590–604.

24. Jia D, Park JH, Jung KH, Levine H, Kaipparettu BA. Elucidating the Metabolic Plasticity of Cancer: Mitochondrial Reprogramming and Hybrid Metabolic States. Cells. 2018;7(3):21.

25. Yu L, Lu M, Jia D, Ma J, Ben-Jacob E, Levine H, et al. Modeling the Genetic Regulation of Cancer Metabolism: Interplay between Glycolysis and Oxidative Phosphorylation. Cancer Res. 2017;77(7):1564–74.

26. Sancho P, Burgos-Ramos E, Tavera A, Bou Kheir T, Jagust P, Schoenhals M, et al. MYC/PGC-1α Balance Determines the Metabolic Phenotype and Plasticity of Pancreatic Cancer Stem Cells. Cell Metab. 2015;22(4):590–605.

27. Jia D, Paudel BB, Hayford CE, Hardeman KN, Levine H, Onuchic JN, et al. Drug-Tolerant Idling Melanoma Cells Exhibit Theory-Predicted Metabolic Low-Low Phenotype. Frontiers Oncol. 2020;10:1426.

28. LeBleu VS, O'Connell JT, Herrera KNG, Wikman H, Pantel K, Haigis MC, et al. PGC-1α mediates mitochondrial biogenesis and oxidative phosphorylation in cancer cells to promote metastasis. Nat Cell Biol. 2014;16(10):992–1003.

29. Dupuy F, Tabariès S, Andrzejewski S, Dong Z, Blagih J, Annis MG, et al. PDK1-Dependent Metabolic Reprogramming Dictates Metastatic Potential in Breast Cancer. Cell Metab. 2015;22(4):577–89.

30. Jia D, Park JH, Kaur H, Jung KH, Yang S, Tripathi S, et al. Towards decoding the coupled decision-making of metabolism and epithelial-to-mesenchymal transition in cancer. Brit J Cancer. 2021;1–10.

31. Georgakopoulos-Soares I, Chartoumpekis DV, Kyriazopoulou V, Zaravinos A. EMT Factors and Metabolic Pathways in Cancer. Frontiers Oncol. 2020;10:499.

32. Fedele M, Sgarra R, Battista S, Cerchia L, Manfioletti G. The Epithelial–Mesenchymal Transition at the Crossroads between Metabolism and Tumor Progression. Int J Mol Sci. 2022;23(2):800.

33. Burger GA, Danen EHJ, Beltman JB. Deciphering Epithelial–Mesenchymal Transition Regulatory Networks in Cancer through Computational Approaches. Frontiers Oncol. 2017;7:162.

34. Hu Y, Xu W, Zeng H, He Z, Lu X, Zuo D, et al. OXPHOS-dependent metabolic reprogramming prompts metastatic potential of breast cancer cells under osteogenic differentiation. Brit J Cancer. 2020;123(11):1644–55.

35. Sung JY, Cheong JH. Pan-Cancer Analysis Reveals Distinct Metabolic Reprogramming in Different Epithelial–Mesenchymal Transition Activity States. Cancers. 2021;13(8):1778.

36. Choudhary KS, Rohatgi N, Halldorsson S, Briem E, Gudjonsson T, Gudmundsson S, et al. EGFR Signal-Network Reconstruction Demonstrates Metabolic Crosstalk in EMT. Plos Comput Biol. 2016;12(6):e1004924.

37. Feng S, Zhang L, Liu X, Li G, Zhang B, Wang Z, et al. Low levels of AMPK promote epithelial-mesenchymal transition in lung cancer primarily through HDAC4- and HDAC5-mediated metabolic reprogramming. J Cell Mol Med. 2020;24(14):7789–801.

38. Kang X, Wang J, Li C. Exposing the Underlying Relationship of Cancer Metastasis to Metabolism and Epithelial-Mesenchymal Transitions. Iscience. 2019;21:754–72.

39. Bocci F, Tripathi SC, Mercedes SAV, George JT, Casabar JP, Wong PK, et al. NRF2 activates a partial epithelial-mesenchymal transition and is maximally present in a hybrid epithelial/mesenchymal phenotype. Integr Biol. 2019;11(6):251–63.

40. Luo M, Shang L, Brooks MD, Jiagge E, Zhu Y, Buschhaus JM, et al. Targeting Breast Cancer Stem Cell State Equilibrium through Modulation of Redox Signaling. Cell Metab. 2018;28(1):69-86.e6.

41. Colacino JA, Azizi E, Brooks MD, Harouaka R, Fouladdel S, McDermott SP, et al. Heterogeneity of Human Breast Stem and Progenitor Cells as Revealed by Transcriptional Profiling. Stem Cell Rep. 2018;10(5):1596–609.

42. Jia D, Li X, Bocci F, Tripathi S, Deng Y, Jolly MK, et al. Quantifying Cancer Epithelial-Mesenchymal Plasticity and its Association with Stemness and Immune Response. J Clin Medicine. 2019;8(5):725.

43. Kovac S, Angelova PR, Holmström KM, Zhang Y, Dinkova-Kostova AT, Abramov AY. Nrf2 regulates ROS production by mitochondria and NADPH oxidase. Biochimica Et Biophysica Acta Bba - Gen Subj. 2015;1850(4):794–801.

44. He F, Ru X, Wen T. NRF2, a Transcription Factor for Stress Response and Beyond. Int J Mol Sci. 2020;21(13):4777.

45. Li N, Muthusamy S, Liang R, Sarojini H, Wang E. Increased expression of miR-34a and miR-93 in rat liver during aging, and their impact on the expression of Mgst1 and Sirt1. Mech Ageing Dev. 2011;132(3):75–85.

46. Bai XY, Ma Y, Ding R, Fu B, Shi S, Chen XM. miR-335 and miR-34a Promote Renal Senescence by Suppressing Mitochondrial Antioxidative Enzymes. J Am Soc Nephrol. 2011;22(7):1252–61.

47. Navarro F, Lieberman J. miR-34 and p53: New Insights into a Complex Functional Relationship. Plos One. 2015;10(7):e0132767.

48. Italiano D, Lena AM, Melino G, Candi E. Identification of NCF2/p67phox as a novel p53 target gene. Cell Cycle. 2012;11(24):4589–96.

49. Chou HL, Fong Y, Wei CK, Tsai EM, Chen JYF, Chang WT, et al. A Quinone-Containing Compound Enhances Camptothecin-Induced Apoptosis of Lung Cancer Through Modulating Endogenous ROS and ERK Signaling. Arch Immunol Ther Ex. 2017;65(3):241–52.

50. Serocki M, Bartoszewska S, Janaszak-Jasiecka A, Ochocka RJ, Collawn JF, Bartoszewski R. miRNAs regulate the HIF switch during hypoxia: a novel therapeutic target. Angiogenesis. 2018;21(2):183–202.

51. Shang Y, Chen H, Ye J, Wei X, Liu S, Wang R. HIF-1α/Ascl2/miR-200b regulatory feedback circuit modulated the epithelial-mesenchymal transition (EMT) in colorectal cancer cells. Exp Cell Res. 2017;360(2):243–56.

52. Byun Y, Choi YC, Jeong Y, Lee G, Yoon S, Jeong Y, et al. MiR-200c downregulates HIF-1α and inhibits migration of lung cancer cells. Cell Mol Biol Lett. 2019;24(1):28.

53. Xu X, Tan X, Tampe B, Sanchez E, Zeisberg M, Zeisberg EM. Snail Is a Direct Target of Hypoxia-inducible Factor 1α (HIF1α) in Hypoxia-induced Endothelial to Mesenchymal Transition of Human Coronary Endothelial Cells*. J Biol Chem. 2015;290(27):16653–64.

54. Chou CC, Lee KH, Lai IL, Wang D, Mo X, Kulp SK, et al. AMPK Reverses the Mesenchymal Phenotype of Cancer Cells by Targeting the Akt–MDM2–Foxo3a Signaling Axis. Cancer Res. 2014;74(17):4783–95.

55. Ohshima J, Wang Q, Fitzsimonds ZR, Miller DP, Sztukowska MN, Jung YJ, et al. Streptococcus gordonii programs epithelial cells to resist ZEB2 induction by Porphyromonas gingivalis. Proc National Acad Sci. 2019;116(17):201900101.

56. Dong T, Zhang Y, Chen Y, Liu P, An T, Zhang J, et al. FOXO1 inhibits the invasion and metastasis of hepatocellular carcinoma by reversing ZEB2-induced epithelial-mesenchymal transition. Oncotarget. 2016;8(1):1703–13.

57. Huang W, Cao J, Liu X, Meng F, Li M, Chen B, et al. AMPK Plays a Dual Role in Regulation of CREB/BDNF Pathway in Mouse Primary Hippocampal Cells. J Mol Neurosci. 2015;56(4):782–8.

58. Jin H, Xue L, Mo L, Zhang D, Guo X, Xu J, et al. Downregulation of miR-200c stabilizes XIAP mRNA and contributes to invasion and lung metastasis of bladder cancer. Cell Adhes Migr. 2019;13(1):236–48.

59. Janin M, Esteller M. Oncometabolite Accumulation and Epithelial-to-Mesenchymal Transition: The Turn of Fumarate. Cell Metab. 2016;24(4):529–30.

60. Zhang Q, Zheng S, Wang S, Wang W, Xing H, Xu S. Chlorpyrifos induced oxidative stress to promote apoptosis and autophagy through the regulation of miR-19a-AMPK axis in common carp. Fish Shellfish Immun. 2019;93:1093–9.

61. Thomson DM, Herway ST, Fillmore N, Kim H, Brown JD, Barrow JR, et al. AMP-activated protein kinase phosphorylates transcription factors of the CREB family. J Appl Physiol. 2008;104(2):429–38.

62. Farris JC, Pifer PM, Zheng L, Gottlieb E, Denvir J, Frisch SM. Grainyhead-like 2 Reverses the Metabolic Changes Induced by the Oncogenic Epithelial–Mesenchymal Transition: Effects on Anoikis. Mol Cancer Res. 2016;14(6):528–38.

63. Radisky DC, Levy DD, Littlepage LE, Liu H, Nelson CM, Fata JE, et al. Rac1b and reactive oxygen species mediate MMP-3-induced EMT and genomic instability. Nature. 2005;436(7047):123–7.

64. Babaei G, Raei N, milani AT, Aziz SGG, Pourjabbar N, Geravand F. The emerging role of miR-200 family in metastasis: focus on EMT, CSCs, angiogenesis, and anoikis. Mol Biol Rep. 2021;48(10):6935–47.

65. SHIDA M, KITAJIMA Y, NAKAMURA J, YANAGIHARA K, BABA K, WAKIYAMA K, et al. Impaired mitophagy activates mtROS/HIF-1α interplay and increases cancer aggressiveness in gastric cancer cells under hypoxia. Int J Oncol. 2016;48(4):1379–90.

66. Thiery JP, Acloque H, Huang RYJ, Nieto MA. Epithelial-Mesenchymal Transitions in Development and Disease. Cell. 2009;139(5):871–90.

67. Zhang K, Zhaos J, Liu X, Yan B, Chen D, Gao Y, et al. Activation of NF-B upregulates Snail and consequent repression of E-cadherin in cholangiocarcinoma cell invasion. Hepato-gastroenterol. 2011;58(105):1–7.

68. Folmes CDL, Nelson TJ, Martinez-Fernandez A, Arrell DK, Lindor JZ, Dzeja PP, et al. Somatic Oxidative Bioenergetics Transitions into Pluripotency-Dependent Glycolysis to Facilitate Nuclear Reprogramming. Cell Metab. 2011;14(2):264–71.

69. Lehuédé C, Dupuy F, Rabinovitch R, Jones RG, Siegel PM. Metabolic Plasticity as a Determinant of Tumor Growth and Metastasis. Cancer Res. 2016;76(18):5201–8.

70. Ramesh V, Brabletz T, Ceppi P. Targeting EMT in Cancer with Repurposed Metabolic Inhibitors. Trends Cancer. 2020;6(11):942–50.

71. Martinez-Outschoorn UE, Peiris-Pagés M, Pestell RG, Sotgia F, Lisanti MP. Cancer metabolism: a therapeutic perspective. Nat Rev Clin Oncol. 2017;14(1):11–31.